Asian Journal of Control, Vol. 18, No. 2, pp. 733–746, March 2016
Published online 20 April 2015 in Wiley Online Library (wileyonlinelibrary.com) DOI: 10.1002/asjc.1110

DYNAMIC STABILITY OF POWER SYSTEMS USING UPFC: BAT-INSPIRED SEARCH AND GRAVITATIONAL SEARCH ALGORITHMS

B. Vijay Kumar and N. V. Srikanth

ABSTRACT

In this paper, the bat-inspired algorithm and the Gravitational Search Algorithm (GSA) based optimal location and capacity of UPFC are proposed to improve the dynamic stability of power systems. The novelty of the proposed method is in improved searching ability, random reduction and reduced complexity. Here, the GSA is used to optimize the location of the UPFC if a generator fault occurs. The GSA selects the maximum power loss line as the optimum location to place UPFC as per the objective function, since the generator fault violates the system equality and inequality constraints from the secure limit. From the UPFC control parameters, the minimum voltage deviation is optimized using the bat algorithm. The minimum voltage deviation has been used to find the optimum capacity of the UPFC. Then the optimum UPFC capacity is applied in the optimum location, which enhances the dynamic stability of the system. The proposed method is implemented in the MATLAB/Simulink platform and the performance is evaluated by means of comparison with the different techniques like GSA and bat-inspired algorithm. The comparison results demonstrate the superiority of the proposed approach and confirm its potential to solve the problem.

Key Words: UPFC, GSA, bat algorithm, power loss, voltage.

I. INTRODUCTION

Electric power systems are required to operate to more or less their own entire capacities worldwide because of the limitations of both their location and the financial resources required to create new generating plants and transmission lines [1,2]. The volume of electric power by security in addition to steadiness restraints, which might be passed among a couple of positions with a transmission network, is limited [3]. Power flow in the lines and transformers really should not be allowed to increase as a haphazard incident may lead to a network collapse as cascaded outages [4,5], resulting in a blockage of the device. The way in which this blockage is handled depends on the rules of the transmission network, which can be driven by powerful forces and, as a result, this becomes the core motion connected with the programs' operators [6]. Studies reveal that insufficient operations connected with transactions can increase congestion costs, which is an additional burden to customers [7].

In relation to handling the power transmission system, Flexible Alternating Current Transmission System (FACTS) is a fixed device that is often employed [8,9]. FACTS may be known as "a power electronic based technique along with other fixed device in which existing control involving one or more AC transmission system parameters formulate controllability and also enlarge power transfer capability" [10]. The various kinds of FACTS devices offered for this specific purpose include Static Var Compensator (SVC), Thyristor controlled series Capacitor (TCSC), Static Synchronous series compensator (SSSC), Static Synchronous Compensator (STATCOM), UPFC and Interlink Power Flow Controller (IPFC) [11]. UPFC is specifically related to FACTS devices, including those that can provide power flow throughout the transmission line by means of effective and also reactive voltage component throughout the chain while using the transmission line [12,13].

Completely new prospects pertaining to handling electrical power in addition to improving the actual utilizable capacity regarding surviving transmission lines are discharged through the look associated with the FACTS equipment [14]. An optimal position regarding the UPFC unit allowing manipulating it is the electrical power systems for an interconnected network, and thus improving the system load ability [15,16]. Otherwise, a new minimized amount of devices, away from which often this load ability can certainly not be improved, continues to be assessed [17]. The optimal position in addition to the optimal capacity of a distinct number of FACTS inside an electrical power process is often an obstacle for combinatorial change [18–20]. A variety of optimization algorithms are actually used to attempt this sort of problem, such as genetic

Manuscript received November 29, 2013; revised May 30, 2014; accepted November 15, 2014.

B. Vijay Kumar (corresponding author) is at the National Institute of Technology, Warangal, India (email: bvijaykumar0478@gmail.com)..

N. V. Srikanth is an Associate Professor, Department of Electrical Engineering, National Institute of Technology, Warangal, India.

algorithms (GA), reproduced annealing (RA), Tabu search (TS), etc [21,22].

In the paper, hybrid technique based dynamic stability of the power system using UPFC is proposed. Here, the GSA optimizes the location of the UPFC, while the generator fault occurs. Location optimization is a process to select the maximum power loss line. Using the optimum location parameters the minimal voltage change is usually achieved by using the bat algorithm. Through the minimum error voltage, most of us find the optimum capacity with the UPFC. Then the optimum UPFC is usually employed within the optimum location and the related results are examined.

II. RECENT RESEARCH WORK: A BRIEF REVIEW

A wide range of studies consider increasing the power transfer capability of power systems, some of which are reviewed in this paper. Shaheen *et al*. have analysed the way the power system security can be improved using UPFC. This improvement can be accomplished by locating the optimum position from the state of line contingency using Differential Evolution (DE) algorithm [23,24]. Taher *et al*. have taken the conditions of a hybrid immune algorithm into account for obtaining the optimal location of UPFCs. Minimization of the cost associated with both the active and the reactive power production of the generators as well as implementation of UPFCs is necessary to get the optimal location [25]. Nireekshana *et al*. [26] have presented a stochastic formulation with Real-code Genetic Algorithm (RGA) to obtain the optimal location and controlling parameters of FACTS devices. Phadke *et al*. [27] have suggested a method, in which Fuzzy logic and Real Coded Genetic algorithm is used for connecting and sizing the shunt FACTS controller. By doing so, the effective area can be measured perfectly using the shunt FACTS devices. Servet *et al*. have proposed a hybrid technique that combines the PSO algorithm and the artificial bee colony (ABC) algorithm for prolonged optimization problems [28]. Kumar *et al*. [29] have dealt with a reliable evolutionary based approach to solve the problems in optimal power flow (OPF). This system hybridises the Fuzzy Systems with GA and PSO algorithm for solving the OPF problem, which is related with the control variables, in an optimal manner.

The review of the recent research work shows that the flows of heavily loaded lines sustain the bus voltages at desired levels and enhances the stability of the power network and increases the uncontrolled exchanges in power systems. For that reason, power systems need to be supervised in sequence to make use of the obtainable network competently. FACTS devices depend on the advance of semiconductor technology released positive latest prospects for controlling the power flow and expanding the loadability of the accessible power transmission system. The UPFC is one of the most promising FACTS devices for load flow control as it can concurrently manage the active and reactive power flow alongside the communication channels in addition to the nodal voltages. As per the characteristics of the UPFC, while scheduling the implementations, it delivers some practical concerns for determining optimal position. In practice, the optimal location of UPFC tends not by randomness, and the matching methodical exploration is not frequently adequate. Previous studies have made an effort to solve the optimal location of UPFCs with respect to different functions and methods. For determining the optimal location, the operating condition of UPFC must be preassigned. Some of the optimization algorithms are introduced to determine the location and size of UPFC such as GA, PSO, DE and etc. This cannot be utilized to find the capacity and location at the same time, so the hybrid approach is needed. These above discussed drawbacks and problems are reduced by using the proposed method.

III. UPFC STRUCTURE AND POWER FLOW MODEL

The UPFC consists of two identical inverters, that is, parallel inverter and series inverter, which are connected in parallel and series to the power systems through the corresponding power transformers. The UPFC is connected between the buses *i* and *j* through the series and parallel power transformers [30,31], the structure of the UPFC is described in Fig. 1. The parallel inverter has been operated either as a voltage controller or a constant reactive power source. It injects constant positive or negative reactive power at i^{th} bus reactive power (Q_i) and regulates the voltage of the bus. The series inverter independently controls the active power (P_j) and reactive power (Q_j) of the j^{th} bus at associated settings, which distinguishes the UPFC from the STATCOM and SSSC. Also the series inverter is used to regulate the

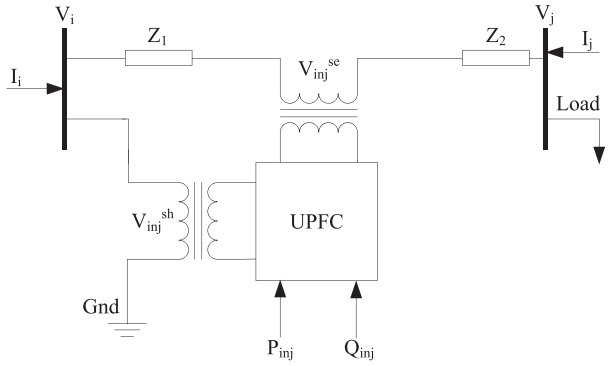

Fig. 1. UPFC installation in power system.

difference between the i^{th} bus voltage (V_i) and j^{th} bus voltage (V_j) bus. The UPFC installation structure of power systems and the equivalent circuit is given in Figs. 1 and 2.

Where, V_{se} and V_{sh} are the magnitudes of injected voltage of the transmission line through the series transformer and shunt transformer, I_{se} and I_{sh} are injected currents with the transmission line through the series transformer and shunt transformer, P_{se} and P_{sh} are the injected powers of the series and shunt transformer, X_{se} and X_{sh} are the reactance values of the series and shunt transformer. From the above equivalent circuit model, the power injection at each node can be derived using the power flow studies. By using the load flow solution, the real and reactive powers on the bus i and j are calculated. The importance of the power injection representation is that the symmetric characteristics of the admittance matrix will not be destroyed [32]. The real and reactive power injection at each bus is described [33] in the following section.

Power flows from i to j:

$$\begin{aligned} P_{ij}(t) = {} & \left(V_i^{2\,(t)} + V_{kl}^{2\,(t)}\right) G_{ij}^{(t)} + 2V_i^{(t)} V_{kl}^{(t)} G_{ij}^{(t)} \cos\left(\alpha_{kl} - \phi_j\right) \\ & - V_j^{(t)} V_{kl}^{(t)} \left[G_{ij}^{(t)} \cos\left(\alpha_{kl} - \phi_j\right) + B_{ij}^{(t)} \left(\sin \alpha_{kl} - \phi_j\right)\right] \\ & - V_i^{(t)} V_j^{(t)} \left(G_{ij}^{(t)} \cos \phi_{ij} + B_{ij}^{(t)} \sin \phi_{ij}\right) \end{aligned} \tag{1}$$

$$\begin{aligned} Q_{ij}(t) = {} & -V_i^{(t)} I^{(t)} - V_i^{2\,(t)} \left(B_{ij}^{(t)} + b/2\right) \\ & - V_i^{(t)} V_{kl}^{(t)} \left[G_{ij}^{(t)} \sin(\alpha_{kl} - \phi_i) + B_{ij}^{(t)} (\cos \alpha_{kl} - \phi_i)\right] \\ & - V_i^{(t)} V_j^{(t)} \left(G_{ij}^{(t)} \sin \phi_{ij} - B_{ij}^{(t)} \cos \phi_{ij}\right) \end{aligned} \tag{2}$$

Where, $G_{ij} + jB_{ij} = \frac{1}{R_{ij} + jX_{ij}}$, V_i and V_j are the voltage of the buses i and j and V_{kl} is the voltage of the compensating device, R_{ij} and X_{ij} are the resistance and reactance between the buses i and j , G_{ij} and B_{ij} are the conductance and susceptance values between the buses i and j respectively, α and ϕ voltage angle and load angle, I is the current value, similarly the real and reactive power flow from the bus j to i is given by the following equations (3) and (4).

Power flows from j to i:

$$\begin{aligned} P_{ji}(t) = {} & V_j^{2\,(t)} G_{ij}^{(t)} + V_j^{(t)} V_{kl}^{(t)} G_{ij}^{(t)} \cos\left(\alpha_{kl} - \phi_j\right) \\ & - B_{ij}^{(t)} G^{(t)} \sin\left(\alpha_{kl} - \phi_j\right) \\ & - V_i^{(t)} V_j^{(t)} \left(G_{ij}^{(t)} \cos \phi_{ij} - B_{ij}^{(t)} \sin \phi_{ij}\right) \end{aligned} \tag{3}$$

$$\begin{aligned} Q_{ji}(t) = {} & V_j^{2\,(t)} \left(B_{ij}^{(t)} + B/2\right) - V_j^{(t)} V_{kl}^{(t)} \\ & \left[G_{ij}^{(t)} \sin\left(\alpha_{kl} - \phi_j\right) - B_{ij}^{(t)} \left(\cos \alpha_{kl} - \phi_j\right)\right] \\ & + V_i^{(t)} V_j^{(t)} \left(G_{ij}^{(t)} \sin \phi_{ij} - B_{ij}^{(t)} \cos \phi_{ij}\right) \end{aligned} \tag{4}$$

The power flow equations are used to identify the capacity of the UPFC, which is evaluated depending on the dynamic stability constraints. The constraints are normally, but whenever a generator fault occurs, they are violated from the stability condition. So the selection of UPFC should satisfy the dynamic stability. The problem formulation of dynamic stability is briefly explained in Section 3.1.

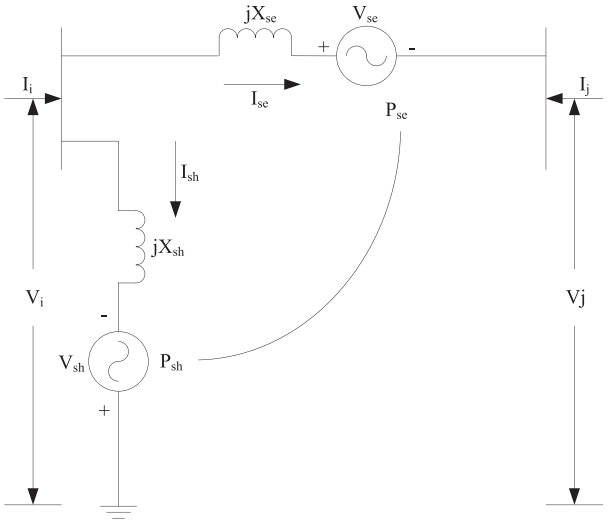

Fig. 2. Equivalent model of UPFC.

3.1 Problem formulation of dynamic stability

Dynamic stability is a nonlinear optimization problem. The primary goal of dynamic stability is to maintain the control variables at the secure limits. The control variables in terms of a certain objective function are subjected to various equality and inequality constraints. The required objective function is mathematically described in the following equations (5), (6) and (7).

$$Minimize\ F(t,u) \tag{5}$$

$$Subject\ to\ g(t,u) = 0 \tag{6}$$

$$h(t,u) \leq 0 \tag{7}$$

Where, $F(t,u)$ is the objective function of the dynamic stability, which minimizes the line loss, voltage deviation and UPFC installation cost, t is the vector dependent variables, u is the dependent variables of the system, g is the equality constraints, h is the operating constraints. The equality and inequality constraints are explained in the following section (i).

(i) Equality constraints

This section describes the equality constraints of the power system. Here, the power system generators need to ensure the customers' total demand and the transmission

loss. It is also known as the power balance condition of the power system. The power system stability condition is affected by the generator outage, which increases the power loss of the system and affects the dynamic stability environment. The required power balance condition can be described in the following equation:

$$\sum_{i=1}^{N_G} P_{Gi} = P_D + \sum_{j=1}^{N_L} \left(P_{Lj} + jQ_{Lj}\right) \tag{8}$$

Where, P_{Gi} is the power generated in the i^{th} bus, P_D is the demand, P_{Lj} and Q_{Lj} are the real and reactive power loss of the j^{th} line, N_G is the total number of generators, N_L is the total number of transmission lines. The real and reactive power loss can be calculated in the following equations [34,35] (9) and (10).

$$P_{Lj} = V_j \sum_{j=1}^{N_B} V_i \left[G_{ji} \cos\left(\delta_j - \delta_i\right) + B_{ji} \sin\left(\delta_j - \delta_i\right)\right] \tag{9}$$

$$Q_{Lj} = V_j \sum_{j=1}^{N_B} V_i \left[G_{ji} \cos\left(\delta_j - \delta_i\right) + B_{ji} \sin\left(\delta_j - \delta_i\right)\right] \tag{10}$$

Where, V_i and V_j are the voltage of the buses i and j, G_{ji} and B_{ji} are the conductance and susceptance between the j^{th} and i^{th} bus, N_B is the total number of buses and δ_i and δ_j are the load angle of the buses i and j. The inequality constraints are explained in the following section (ii).

(ii) Inequality constraints

This section describes the inequality constraints of the power system, that is, voltage, real and reactive power flow. These constraints should be maintained at the stability limit, because the dynamic stability mainly considers the voltage stability of every node. The stable voltage limit of the every node may be *0.95 to 1.05 pu*. The change in voltage can be described by the following equations:

$$\Delta V_i = \frac{1}{\sqrt{l}} \sqrt{\sum_{i=1}^{l} \left(V_i^k\right)^2} \tag{11}$$

Where,

$$V_i^k = V_{slack} - \sum_{i=1}^{n} Z_i \left(\frac{P_i - jQ_i}{V_i}\right) \tag{12}$$

With, V_{slack} is the slack bus voltage, ΔV_i is the voltage stability index of the bus i, V_i is voltage of the bus, where $i = 1, 2, 3 \ldots n$, l is the number of nodes, Z_i is the impedance of the i^{th} bus, P_i and Q_i are the real and reactive power of bus i and j is the number of nodes. The bus voltage lies between the limits, that is, $V_i^{\min} \le V_i \le V_i^{\max}$. The real and reactive power of the i^{th} bus can be described by the following equations (6) and (7).

$$P_i = |V_i||V_j| \sum_{j=1}^{N_B} \left(G_{ij} \cos \delta_{ij} + B_{ij} \sin \delta_{ij}\right) \tag{13}$$

$$Q_i = |V_i||V_j| \sum_{j=1}^{N_B} \left(G_{ij} \sin \delta_{ij} - B_{ij} \cos \delta_{ij}\right) \tag{14}$$

Where, V_i and V_j are the voltage of i and j buses respectively, N_B is the total number of buses, δ_{ij} and δ_{ij} are the angle between i and j buses respectively, G_{ij} and B_{ij} are the conductance and susceptance values respectively. During the generator fault condition, the power flow constraints are affected, which causes instability in the system. In these conditions, dynamic stability is achieved by selecting the optimum location and capacity of the UPFC using the proposed method. The proposed method is briefly explained in the following Section 3.2.

3.2 Hybrid Technique Based Dynamic Stability

3.2.1 Optimum location determination using GSA

This section describes the GSA based optimum location determination. Initially the IEEE standard benchmark system normal power flow is analyzed using the N-R load flow analysis. Then the generator fault is introduced in the bus system, so the bus system becomes unstable. Here, the GSA technique is used to find the most affected location to place the UPFC, that is, maximum power loss line. The maximum power loss line is the most suitable location to fix the UPFC. At the beginning the input agents like voltage at each bus and the power loss at each line is randomly generated with the required n dimensions search space. The random generated agents are given in the following equation (15).

$$X_i = \left[(V_1, P_{L1})^1, (V_2, P_{L2})^2, (V_3, P_{L3})^3 \ldots (V_n, P_{Ln})^n\right] \tag{15}$$

Where, $(V_i, P_{Li})^d = X_i^d$ defines the position of the i^{th} agent at d^{th} dimension. The random generated agents are used to calculate the optimum location, which is described in the following relation (16).

$$\Phi = Max\left\{ V_j \sum_{j=1}^{N_B} V_i \left[G_{ji} \cos\left(\delta_j - \delta_i\right) + B_{ji} \sin\left(\delta_j - \delta_i\right)\right] \right\} \tag{16}$$

According to Newton's gravitation theory the total force acts on the agent as described in the following equation (17).

$$force_i^d(t) = \sum_{j \neq i} rand_j \left(force_{ij}^d(t) \right) \quad (17)$$

Where, $force_{ij}^d(t) = G(t) \frac{M_{pi}(t) * M_{aj}(t)}{R_{ij} + \varepsilon} * \left(X_j^d(t) - X_i^d(t) \right)$

with, $R_{ij} = ||X_i(t), X_j(t)||_2$ is the Euclidian distance between two agents i and j, $rand_j$ is the random values, that is, [0, 1], ε is a small constant, M_{aj} and M_{pi} active and passive gravitational mass related to agent i and j. Here, the acceleration of the i^{th} agent can be determined by the following equation.

$$Acceleration\ a_i^d(t) = \frac{force_i^d(t)}{M_i(t)}$$

Update the agent's position, using the following velocity equation (18).

$$V_i^d(t+1) = rand_i . \left[V_i^d \right] + a_i^d(t) \quad (18)$$

The above velocity function is used to develop the new agents, which can be described in the following equation (19).

$$X_i^d(t+1) = X_i^d(t) + V_i^d(t+1) \quad (19)$$

Where, $V_i^d(t)$ and $X_i^d(t)$ are the velocity and position of an agent at t time and d dimension, $rand_i$ is the random number in the interval [0, 1]. The steps to find the optimum location are given in the following section.

(a) Steps to find the optimum location

Step 1: In the first step, the input agents are randomly generated at N dimensions. Here, the bus voltage and the line losses are selected as the agents.

Step 2: Apply load flow solution and then, evaluate the fitness values of the random number of agents.

Step 3: In the high mass, agents are selected as the best solutions and the corresponding load flow is analyzed.

Step 4: The best solutions are separated into two groups, the first groups have the minimum best solutions and another group has maximum best solutions.

Step 5: For each best solution groups, the agent's positions and velocity are modified.

Step 6: Run load flow analysis and evaluate the new agents. Select the best agent from each group.

Step 7: Find the voltage, real and reactive power flow and power loss.

Step 8: Check the termination criterion. If it is satisfied terminate or go to step 9.

Step 9: Generate the new agents to generate new solutions. Go to Step 2.

Once the process is finished, the GSA is ready to give the optimal location of the UPFC.

3.2.2 UPFC capacity determination using bat algorithm

The bat inspired algorithm is the optimization algorithm, which works based on the echolocation behavior of bats [36]. Here, the bat inspired algorithm is used to optimize the capacity of the UPFC. Initially the bus voltage for both the normal condition and the fault condition is being reduced by the required objective function. The minimum error voltage and the maximum error voltage are classified according to the objective function. The minimum voltage deviation attaining UPFC capacity is optimum capacity. By using the optimum UPFC capacity, the dynamic stability of the system is enhanced. The steps to optimize the capacity of the UPFC are described below.

(a) Steps to find the UPFC optimum capacity

Step 1: Input micro-bats (B_i) population is randomly generated, that is, IEEE standard benchmark system bus voltage and the UPFC power flow equations, which should satisfy the power balance condition. Each micro-bat has the velocity vector (v_i) and position vector (x_i), which is described in the following equation (20).

$$B_i = \left[(v_{12}, x_{12})^{b1} \quad (v_{12}, x_{12})^{b2} \quad \ldots \quad (v_{12}, x_{12})^{bn} \right] \quad (20)$$

Step 2: To assign the echolocation parameters, the micro-bat populations are incorporated with the echolocation parameters like frequency (f_i), pulse rate (r_i) and the loudness parameters (l_i). These parameters are non-negative real values with the following ranges.

$$f_{\min} \leq f_i \leq f_{\max} \quad (21)$$

$$r_{\min} \leq r_i \leq r_{\max} \quad (22)$$

$$l_{\min} \leq l_i \leq l_{\max} \quad (23)$$

Here, we assign the frequency range $f_{\min} = 0$ and $f_{\max} = 1$, the pulse rate minimum value is $r_{\min} = 0.5$ and the loudness maximum value is $l_{\max} = 1$. The remaining values are determined by the following equation (24).

$$l_{\min} = \frac{1}{\sqrt{n_{\sec}}} \text{ and } r_{\max} = 1 - \frac{1}{n_d} \leq 1 \quad (24)$$

Where, $n_{\sec}$ is the number of sections in the discrete set used for sizing the design variable and $n_{\sec}$ is the number of discrete design variables.

Step 3: Evaluate the objective function of the initial populations; the required objective function is described in the following equation (25).

$$\Psi = Min\sum_{i=1}^{N_B}\left(V_{Normal} - V_i^F\right) \tag{25}$$

Where, V_{Normal} is the bus voltage at normal condition and V_i^F is the bus voltage at different types of generator fault condition.

Step 4: Store the current population and increase the iteration count as $t+1$, that is, iteration $t=t+1$.

Step 5: The current population of bus voltages are randomly updated based on the frequency and the velocity. Initially the frequency can be evaluated, which is described in the following equation (26).

$$f_i^t = f_{\min} + (f_{\max} - f_{\min})u_i \tag{26}$$

Where there is a random number of values, which is selected from 0 to 1, then the frequency is applied into the velocity equation, which can be described in the following equation (27).

$$v_i^t = round\ \left[v_i^{t-1} + \left(X_i^{t-1} - X_\Psi\right)u_i\right] \tag{27}$$

Where, v_i^t and v_i^{t-1} are the velocity vectors of the micro-bats at the time steps t and $t-1$, X_i^t and X_i^{t-1} are the position vectors of the micro-bats at time steps t and $t-1$, X_Ψ is the current global best solution. Hereafter the local search is performed on the randomly selected population that is described in the following equation (28).

$$x_i^t = x_i^{t-1} + \xi_{i,j} l_{avg}^t \tag{28}$$

Where, $\xi_{i,j}$ is a random number between -1 and 1, l_{avg}^t is the average value of loudness at time step t.

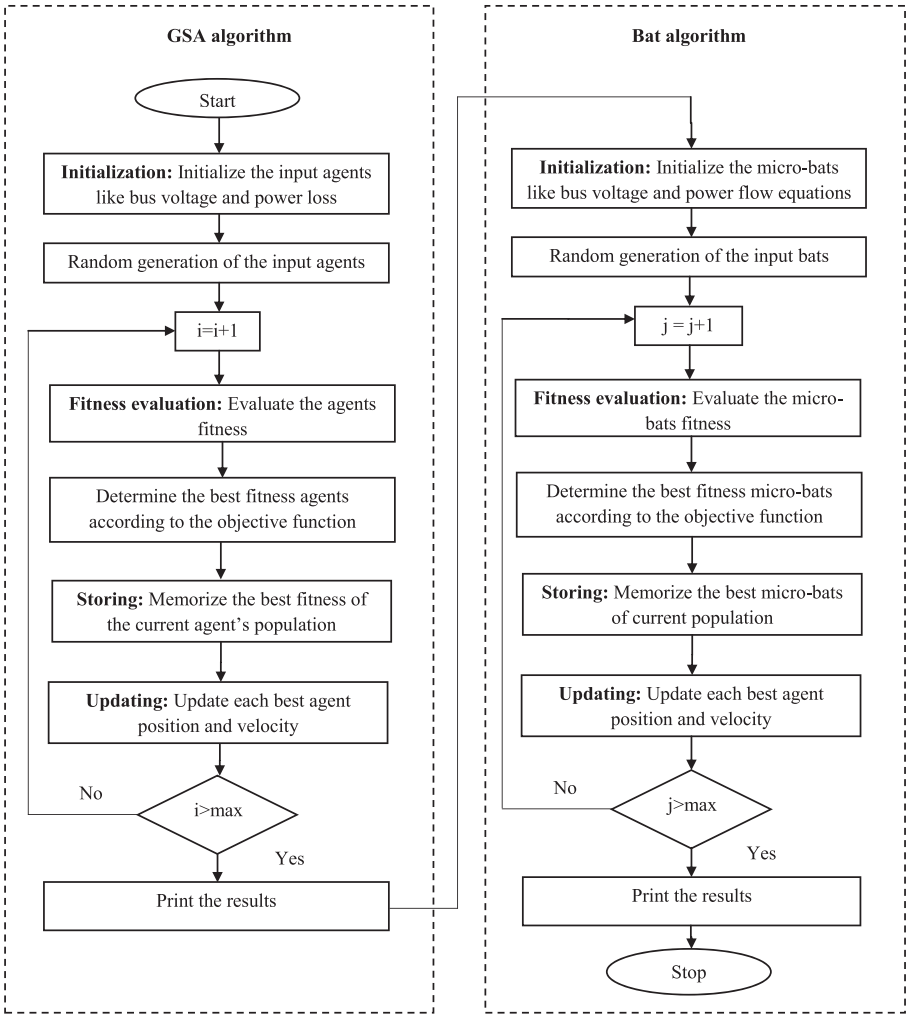

Fig. 3. Structure of the proposed method.

Step 6: Find the fitness of the new micro-bats population using the equation (28). After evaluation, the micro-bats echolocation parameters are updated for better movement of the micro-bats, which can be described in the following equation (29).

$$l_i^{'} = a.l_i \text{ and } r_i^{t+1} = r_{\max}[1 - \exp(\gamma t)] \quad (29)$$

Where, $l_i^{'}$ and l_i are the previous and updated values of the loudness, r^{t+1} is the pulse rate of the micro-bats in time step , a and γ are the adaptation parameters of the loudness and pulse rate.

Step 7: To find the best micro-bats, which satisfy the objective function (25).

Step 8: The steps 4 to 7 are continued until the termination criteria is attained.

Once the termination criterion is attained, the system is ready to give the optimum capacity of the UPFC. The selected capacity is utilized in the appropriate location and analyzes the load flow solution; it may enhance the dynamic stability of the system. The proposed method structure is illustrated in Fig. 3. The proposed method is tested on the MATLAB platform and the numerical results are analyzed with various techniques, which are briefly described in the next section 4.

IV. RESULTS AND DISCUSSIONS

The proposed method is implemented in MATLAB/Simulink 7.10.0 (R2012a) platform, 4GB RAM and Intel(R) core(TM) i5. Here the IEEE 30 bus system and 14 bus systems are used to validate the proposed method. The numerical results of the proposed method are presented and discussed in this section. The effectiveness of the proposed method is analyzed by comparing with those of other techniques such as Genetic Algorithm (GA), GSA algorithm and bat inspired algorithm. The proposed method is applied in the IEEE 30 bus system and discussed in the following Section 4.1.

4.1 Validation of IEEE 30 bus systems

The proposed method is tested in the IEEE 30 bus system and the corresponding numerical results are discussed in this section. The IEEE 30 bus system consists of 6 generator bus, 21 load bus and 42 transmission lines. Initially the normal load flow of the bus system is analyzed using the N-R load flow method; afterwards the generator fault is introduced into the bus system. The instability condition is determined and solved using the proposed method. Here, the power flow analysis and power loss of the IEEE 30 bus system at normal condition, single generator fault condition and using the proposed method are described in Tables I and II respectively. Then the voltage profile for each generator outage is discussed in the following section.

The bus voltage profile during the generator outage at the second bus is illustrated in Fig. 4. From that we observe that the bus voltage is maintained at the stability limit during the normal power flow condition, that is, in the N-R method, the voltage profile faces the instability during the second generator outage. Then the voltage instability is reduced by optimizing the location and capacity of the UPFC using the proposed method. At the sixth bus generator outage using the proposed method is

Table II. Power loss at single generator problem using the proposed method.

Generator bus no.	Best location		Power loss in MW		
	From bus	To bus	Normal	Generator outage	With UPFC
2	12	15	10.809	12.768	8.718
6	5	7		12.552	8.087
13	12	15		12.795	8.536
22	10	22		11.883	8.063
27	22	24		11.903	8.517

Table I. Power flow analysis at single generator problem using the proposed method.

Generator bus no.	Best location		Power flow					
			Normal		Generator outage		With UPFC	
	From bus	To bus	P (MW)	Q (MVAR)	P (MW)	Q (MVAR)	P (MW)	Q (MVAR)
2	12	15	19.675	7.796	19.797	7.755	20.491	2.378
6	5	7	23.744	13.825	24.763	14.248	20.113	17.702
13	12	15	19.675	7.796	19.797	7.755	20.524	4.184
22	10	22	4.047	6.617	4.044	6.581	2.767	2.967
27	22	24	7.913	3.145	9.714	1.940	8.592	3.209

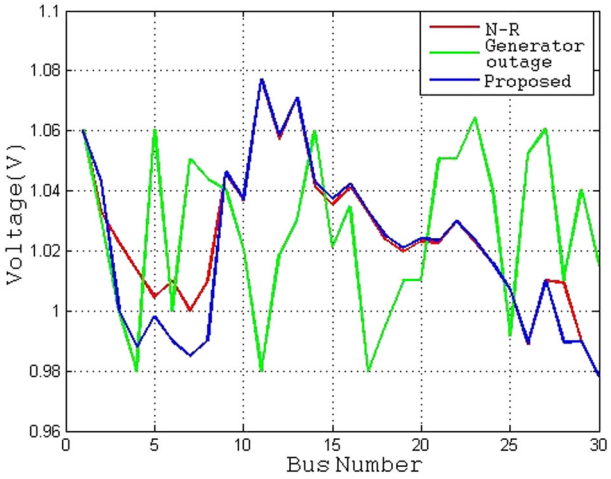

Fig. 4. Voltage profile during generator outage at 2nd bus.

illustrated in Fig. 5. Similarly the other generators such as 13, 22 and 27 are turned off at different environments. The corresponding voltage stability is analyzed in Figs. 6, 7 and 8 respectively.

The IEEE 30 bus system generators are turned off at different time intervals, which is a single generator problem. At these different environments, the total power loss of the IEEE bench mark system has been measured. The single generator fault power loss problem is resolved by using the proposed hybrid method. The power loss measurement of the single generator problem is shown in Table II. It shows the performance of the proposed method, because the power loss has been reduced compared to the normal time and the fault condition. Then the IEEE 30 bus system is allowed to meet the double generator problem. By this time the two generator problem has occurred at different intervals and the corresponding power flow is shown in Table III.

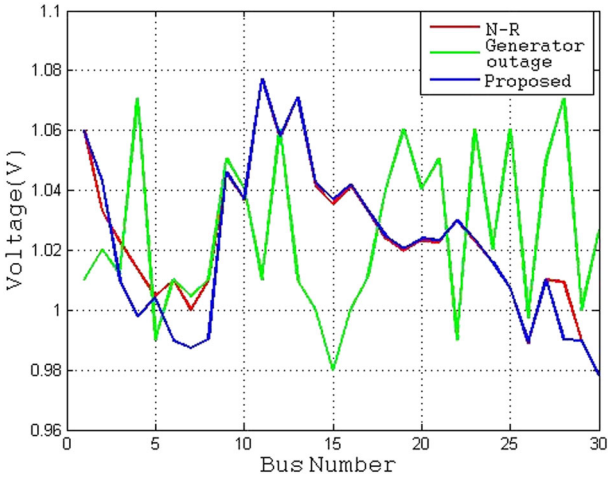

Fig. 5. Voltage profile during generator outage at 6th bus.

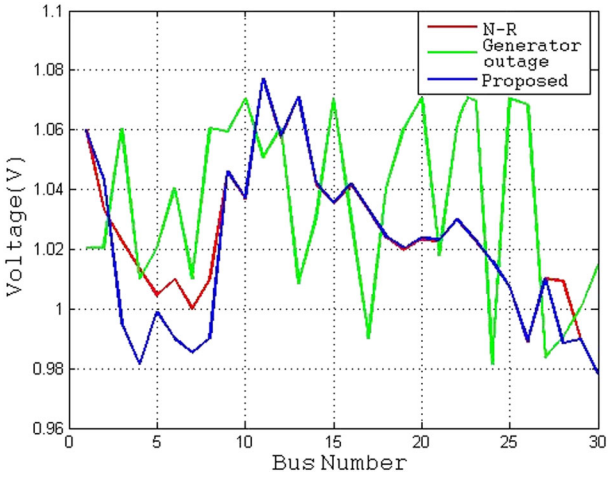

Fig. 6. Voltage profile during generator outage at 13th bus.

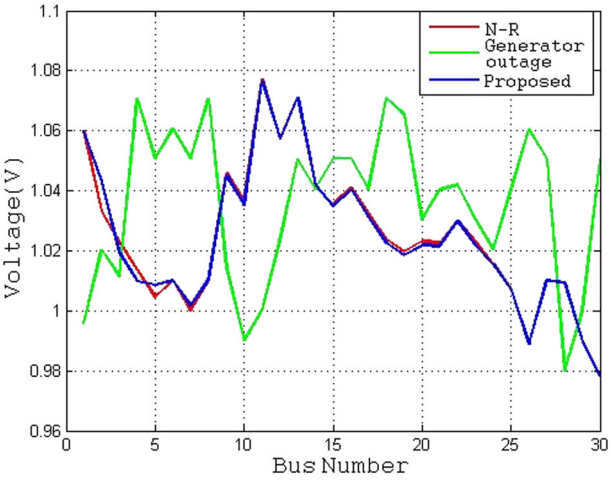

Fig. 7. Voltage profile during generator outage at 22nd bus.

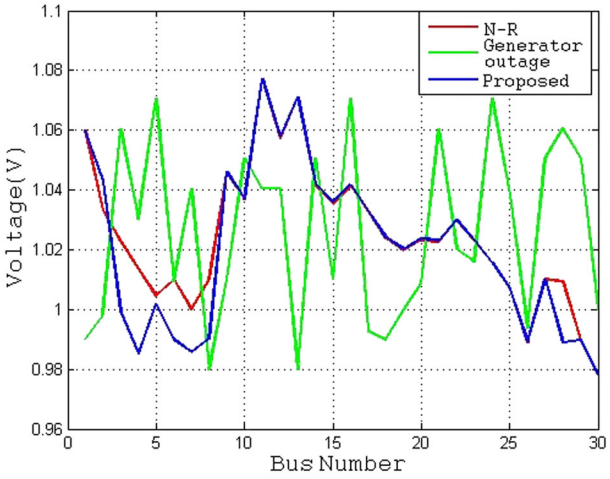

Fig. 8. Voltage profile during generator outage at 27th bus.

Table III. Power flow analysis at double generator problem using the proposed method.

Generator bus no.	Best location		Power flow					
			Normal		Generator outage		With UPFC	
	From bus	To bus	P (MW)	Q (MVAR)	P (MW)	Q (MVAR)	P (MW)	Q (MVAR)
2 and 6	10	22	1.047	6.617	4.044	6.581	0.325	2.343
2 and 13	5	7	23.744	13.825	24.763	14.248	20.971	15.571
6 and 13	15	23	5.893	3.546	2.003	4.598	5.421	3.731
22 and 27	12	15	19.675	7.796	19.797	7.755	20.193	7.908
13 and 27	2	5	72.803	2.549	77.585	2.087	77.626	2.096

The double generator problem power loss is illustrated in Table IV. The voltage profile variation according to the double generators shut down condition is explained in Figs. 9–13. Here, the voltage profile is compared at various conditions, that is, normal condition, during fault condition and by means of the proposed method. The normal voltage profile exceeds the stability limit, as the generator fault conditions. Depending on the fault range the proposed method identifies the UPFC location and capacity, which is used to resolve the voltage instability problem.

Table IV. Power loss at double generator problem using the proposed method.

Generator bus no.	Best location		Power loss in MW		
	From bus	To bus	Normal	Generator outage	With UPFC
2 and 6	10	22	10.809	14.731	8.536
2 and 13	5	7		15.017	8.795
6 and 13	15	23		14.833	8.725
22 and 27	12	15		13.051	8.282
13 and 27	2	5		14.005	8.130

The normal power loss of the IEEE 30 bus system is 10.809, which is increased during the double generator problem. The maximum power loss is reduced by locating the optimum capacity of UPFC using the proposed method.

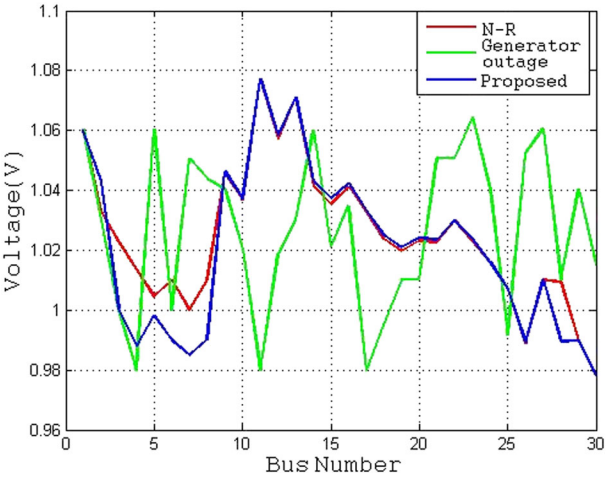

Fig. 10. Voltage profile during generator outage at buses 2 and 13.

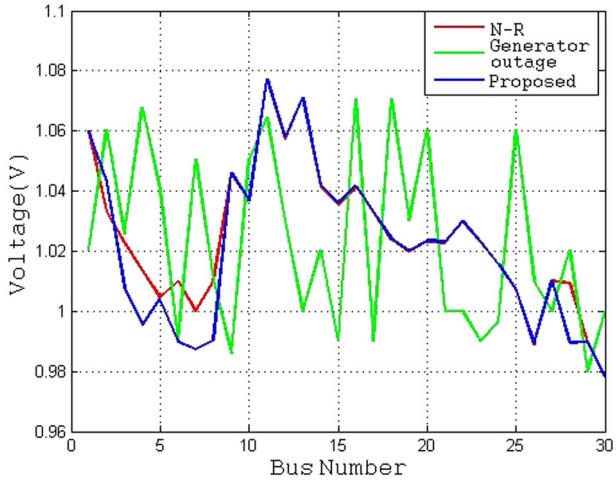

Fig. 9. Voltage profile during generator outage at buses 2 and 6.

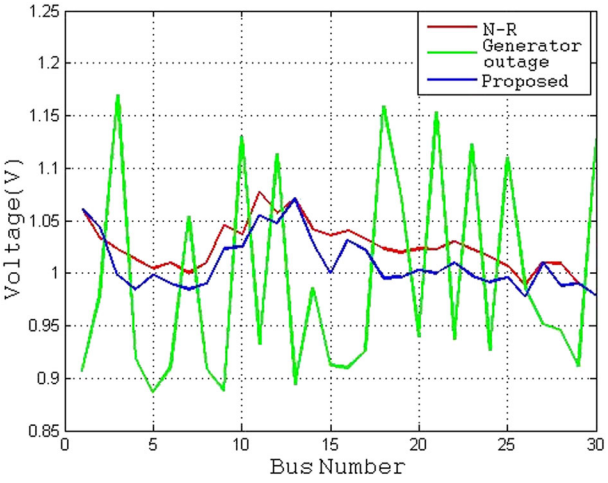

Fig. 11. Voltage profile during generator outage at buses 6 and 13.

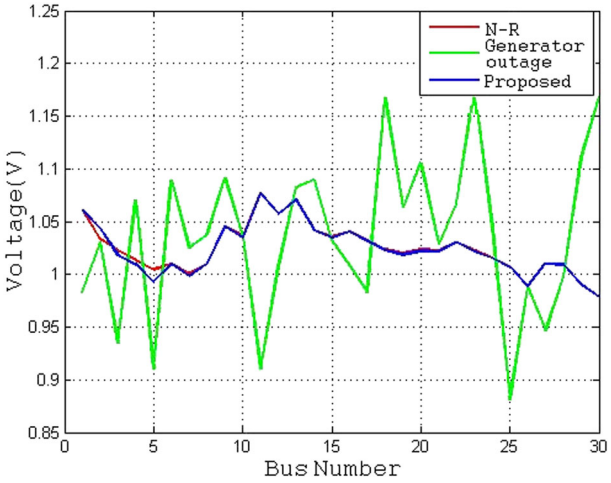

Fig. 12. Voltage profile during generator outage at buses 13 and 27.

The double generator problem power loss comparison is described in Table IV. The proposed method effectiveness is analyzed by comparing the proposed method numerical results with those of the other techniques such as the GA, GSA algorithm and bat inspired algorithm. The IEEE 30 bus systems with the single generator problem power flow comparison using different techniques are explained in Table V. Similar conditions of the power loss comparison with different techniques are described in Table VI.

The voltage profile of the IEEE 30 bus system at a single generator problem using different techniques is explained in Fig. 14. The existing optimization techniques struggle because of their weak local search and unreasonable random generation. Therefore, the existing optimization techniques give poor solutions to the dynamic stability problem. From that we conclude that the proposed method effectively selects the optimum location and capacity of the UPFC compared to the other optimization techniques, because the proposed method actively maintains dynamic stability of the IEEE 30 bus test system, that is,

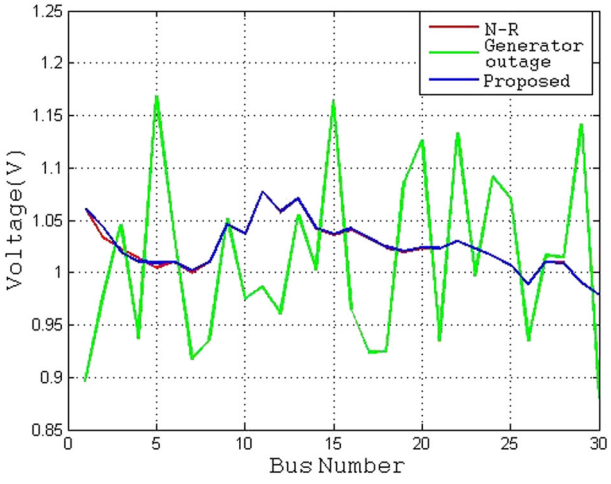

Fig. 13. Voltage profile during generator outage at buses 22 and 27.

Table VI. Power loss comparison at single generator problem using different techniques.

Fault Generator bus no.	Best location		Power loss in MW				
	From bus	To bus	Normal	GA	GSA	Bat	Proposed
2	12	15	10.809	9.854	9.122	8.866	8.718

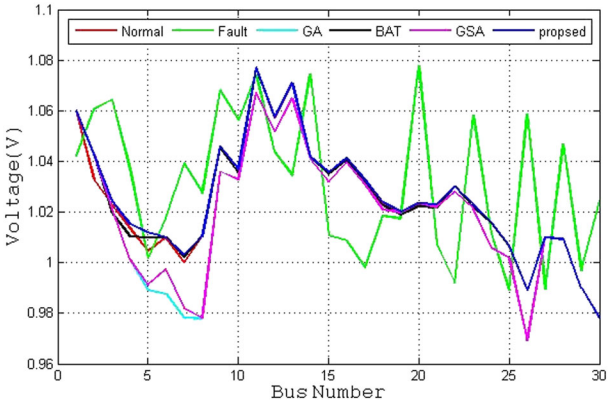

Fig. 14. Voltage profile comparison at single generator outage.

Table V. Power flow comparison at single generator problem using different techniques.

Technique	Fault Generator bus no.	Best location		Power flow during normal condition		Power flow during fault condition		Power flow after fixing the UPFC	
		From bus	To bus	P (MW)	Q (MVAR)	P (MW)	Q (MVAR)	P (MW)	Q (MVAR)
GA	2	12	15	19.675	7.796	19.797	7.755	23.225	5.655
GSA	2	12	15					21.585	5.473
Bat	2	12	15					20.857	6.338
Proposed	2	12	15					20.491	2.378

maintains the voltage profile at the stability limit and reduces the power loss (8.718 MW). The proposed method effectiveness is also verified by using the IEEE 14 bus system, which is briefly discussed in the following Section 4.2.

4.2 Validation of IEEE 14 bus system

This section describes the proposed method, which is applied in the IEEE 14 bus system consisting of 2 generator buses, that is, one generator in slack bus and another one on the second bus. The load flow solution at normal condition is determined using the N-R load flow analysis, which identifies all the system constraints like bus voltage, power loss, etc. Here, we turn off the generator at the second bus. At this time the power flow meets the difficulties, which is resolved by identifying the problem location and fixing optimum capacity of the UPFC. The power flow comparisons at single generator problem using different techniques are described in Table VII. The power loss comparison is illustrated in Table VIII.

The voltage profile of the IEEE 14 bus system using different techniques at a single generator problem is described in Fig. 15. From that, the voltage profile is actively maintained at the stability limit by using the proposed method compared to the other techniques. The power loss of the IEEE 14 bus system is effectively reduced at 10.275 MW using the proposed method, which is better compared to the GA, GSA and bat algorithms. Fig. 16 illustrates the bus voltage profile comparison between different techniques like N-R method, DG off time and the proposed method. Here, the proposed method effectively maintains the voltage profile within the mentioned limit (0.95 pu to 1.05 pu). The computation time and the performance of the proposed algorithm are better than those of the GA, GSA and bat optimization algorithms for these two problems, which are described in Fig. 17. The GA has high number of computation time among the represented optimization algorithms. The computational time of the bat-inspired algorithm is 6.990256 seconds and 20.028565 seconds for IEEE 14 and 30 bus system respectively. The GSA has the computational time for IEEE 14 bus system as 7.067493 seconds and for IEEE 30 bus system it is 13.531510 seconds. Thus, the proposed method reduces the computational time compared to the other explained techniques. From the comparison results obtained, we can conclude that the proposed method is an effective method to maintain the dynamic stability of the power system compared to the other techniques.

Table VIII. Power loss comparison using different techniques.

Fault Generator bus no.	Selected lines		Power loss in MW				
	From bus	To bus	Normal	GA	GSA	Bat	Proposed
2	4	5	13.592	12.224	11.765	11.547	10.275

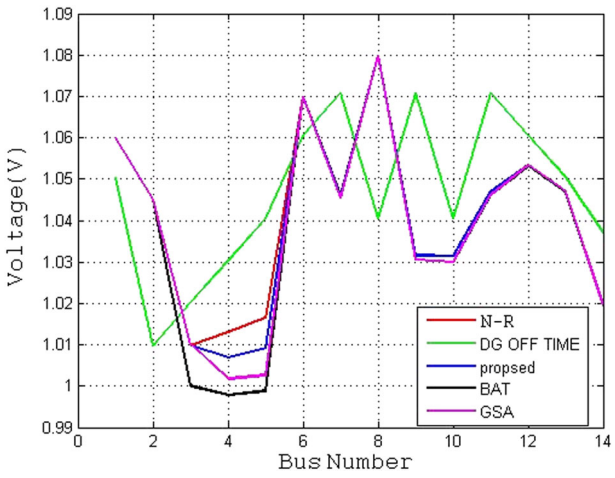

Fig. 15. Voltage profile comparison at single generator problem.

V. CONCLUSION

This paper proposes a hybrid technique based dynamic stability of the power system using UPFC. Here, the maximum power loss line is optimized by using the GSA technique and the optimum capacity of the UPFC is

Table VII. Power flow comparison using different techniques.

Technique	Fault Generator bus no.	Best location		Power flow during normal condition		Power flow during fault condition		Power flow after fixing the UPFC	
		From bus	To bus	P (MW)	Q (MVAR)	P (MW)	Q (MVAR)	P (MW)	Q (MVAR)
GA	2	4	5	59.585	11.574	62.894	14.208	58.369	9.994
GSA	2	4	5					56.287	9.827
Bat	2	4	5					55.796	9.948
Proposed	2	4	5					52.030	10.148

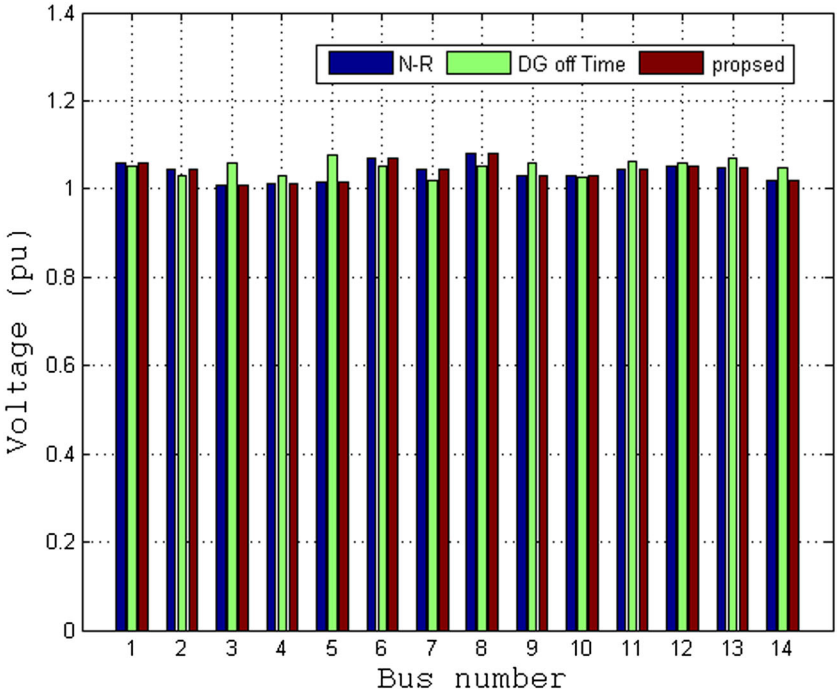

Fig. 16. Voltage profile comparison in bar chart.

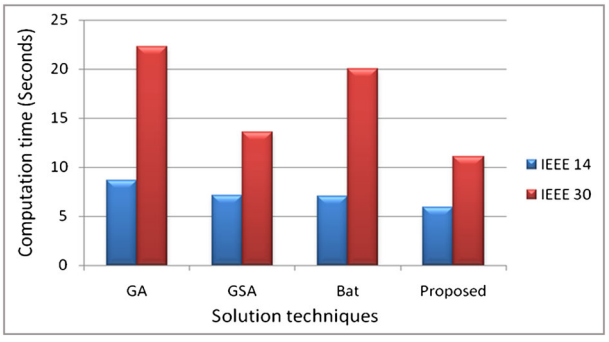

Fig. 17. Computational time comparison.

determined by using the bat inspired algorithm. The advantage of the proposed method is the improved searching ability to solve complex problems and enhance reliability. The proposed hybrid method is tested under the IEEE 30 bus system and IEEE 14 bus system at different types of generator faults. During the generator fault condition, bus system voltage profile and power loss are analyzed at normal conditions by the GSA algorithm, bat inspired algorithm and the proposed hybrid technique. The obtained numerical results are compared and the performances discussed. From these comparison results we conclude that the proposed hybrid technique is effective for maintaining the dynamic stability of the power system, more so than other techniques.

REFERENCE

1. Ramasubramanian, P., G. Uma Prasana, and K. Sumathi, "Optimal location of FACTS devices by evolutionary programming based OPF in deregulated power systems," *British J. Math. Comput. Sci.*, Vol. 2, No. 1, pp. 21–30 (2012).
2. Lubis, R. S., S. P. Hadi, and Tumiran, "Selection of suitable location of the FACTS devices for optimal power flow." *Int. J. Electr. Comput. Sci.*, Vol. 12, No. 3, pp. 38–49 (2012).
3. Durairaj, S., and B. Fox, "Optimal placement of facts devices." *International Conference on Energy & Environment* (2008).
4. Devaraj, D., and J. Preetha Roselyn, "Genetic algorithm based reactive power dispatch for voltage stability improvement," *Int. J. Electr. Power Energy Syst.*, Vol. 32, No. 10, pp. 1151–1156 (2010).
5. Chaohua, D., C. Weirong, Z. Yunfang, and Z. Xuexia, "Reactive power dispatch considering voltage stability with seeker optimization algorithm," *Electr. Power Syst. Res.*, Vol. 79, No. 10, pp. 1462–1471 (2009).
6. Khazali, A. H., and M. Kalantar, "Optimal reactive power dispatch based on harmony search algorithm." *Int. J. Electr. Power Energy Syst.*, Vol. 33, No. 3, pp. 684–692 (2011).
7. Raoufi, H., and M. Kalantar, "Reactive power rescheduling with generator ranking for voltage

stability improvement," *Energy Conv. Manag.*, Vol. 50, No. 4, pp. 1129–1135 (2009).
8. Shimpi, R. J., R. P. Desale, K. S. Patil, J. L. Rajput, and S. B. Chavan, "Flexible AC transmission systems," *Int. J. Comput. Appl. Technol.*, Vol. 1, No. 15, pp. 54–57 (2010).
9. Dash, P. K., S. R. Samantaray, and G. Panda, "Fault classification and section identification of an advanced series-compensated transmission line using support vector machine," *IEEE Trans. Power Deliv.*, Vol. 22, No. 1, pp. 67–73 (2007).
10. Bansal, H. O., H. P. Agrawal, S. Tiwana, A. R. Singal, and L. Shrivastava, "Optimal location of FACT devices to control reactive power," *Int. J. Eng. Sci. Technol.*, Vol. 2, No. 6, pp. 1556–1560 (2010).
11. Murali, D., and M. Rajaram, "Active and reactive power flow control using FACTS Devices," *Int. J. Comput. Appl.*, Vol. 9, No. 8, pp. 45–50 (2010).
12. Wei, X., J. H. Chow, B. Fardanesh, and A. Edris, "A common modeling framework of voltage–sourced converters for load flow, sensitivity, and dispatch analysis," *IEEE Trans. Power Syst.*, Vol. 19, No. 2, pp. 934–941 (2004).
13. Ravi Kumar, S. V., and S. Siva Nagaraju, "Functionality of UPFC in stability improvement," *Int. J. Electr. Power Eng.*, Vol. 1, No. 3, pp. 339–348 (2007).
14. Sarda, J. S., V. N. Parmar, D. G. Patel, and L. K. Patel, "Genetic algorithm approach for optimal location of FACTS devices to improve system loadability and minimization of losses," *Int. J. Adv. Res. Electr., Electr. Instrum. Eng.*, Vol. 1, No. 3, pp. 114–125 (2012).
15. Gerbex, S., R. Cherkaoui, and A. J. Germond, "Optimal location of FACTS devices to enhance power system security." *IEEE Bologna Power Tech Conference Proceedings* (2003).
16. Pujol, G. and L. Acho, "Active control for a perturbed flexible structure: an experimental study," *Asian J. Control*, Vol. 15, No. 6, pp. 1566–1570 (2013).
17. Mori, H., and Y. Goto, "A parallel tabu search based method for determining optimal allocation of FACTS in power systems." *International Conference on Power System Technology* (2000).
18. Feng, W., and G. B. Shrestha, "Allocation of TCSC devices to optimize total transmission capacity in a competitive power market." *IEEE Power Engineering Society Winter Meeting* (2001).
19. Vaidya, P.S., and V. P. Rajderkar, "Optimal location of series FACTS devices for enhancing power system security." *4th International Conference on Emerging Trends in Engineering and Technology* (2011).
20. Mahdad, B., T. Bouktir, and K. Srairi, "GA coordinated with practical fuzzy rules with multi shunt FACTS devices to enhance the optimal power flow." *The International Conference on Computer and Tool* (2007).
21. Cai, L.J., I. Erlich, and G. Stamtsis, "Optimal choice and allocation of FACTS devices in deregulated electricity market using genetic algorithms." *IEEE PES Power Systems Conference and Exposition* (2004).
22. Ortega, C., A. Arias, and J. Espina, "Predictive direct torque control of matrix converter fed permanent magnet synchronous machines," *Asian J. Control*, Vol. 16, No. 1, pp. 70–79 (2014).
23. Shaheen, H. I., G.I. Rashed, and S.J. Cheng, "Application and comparison of computational intelligence techniques for optimal location and parameter setting of UPFC," *Eng. Appl. Artif. Intel.*, Vol. 23, pp. 203–216 (2010).
24. Shaheen, H. I., G. I. Rashed, and S. J. Cheng, "Optimal location and parameter setting of UPFC for enhancing power system security based on Differential Evolution algorithm," *Electr. Power Energy Syst.*, Vol. 33, pp. 94–105 (2011).
25. Taher, S. A., and M. K. Amooshahi, "New approach for optimal UPFC placement using hybrid immune algorithm in electric power systems," *Electr. Power Energy Syst.*, Vol. 43, pp. 899–909 (2012).
26. Nireekshana, T., G. Kesava Rao, and S. Siva Naga Raju, "Enhancement of ATC with FACTS devices using Real-code Genetic Algorithm," *Electr. Power Energy Syst.*, Vol. 43, pp. 1276–1284 (2012).
27. Phadke, A. R., and M. F. K.R. Niazi, "A new multi-objective fuzzy-GA formulation for optimal placement and sizing of shunt FACTS controller," *Int. J. Electr. Power Energy Syst.*, Vol. 40, No. 1, pp. 46–53 (2012).
28. Kiran, M. S. and M. Gunduz, "A recombination-based hybridization of particle swarm optimization and artificial bee colony algorithm for continuous optimization problems," *Appl. Soft Comput.*, Vol. 13, No. 4, pp. 2188–2203 (2013).
29. Kumar, S., and D.K. Chaturvedi, "Optimal power flow solution using fuzzy evolutionary and swarm optimization," *Int. J. Electr. Power Energy Syst.*, Vol. 47, pp. 416–423 (2013).
30. Rajabi-Ghahnavieh, A., M. Fotuhi-Firuzabad, M. Shahidehpour, and R. Feuillet, "UPFC for enhancing power system reliability," *IEEE Trans. Power Deliv.*, Vol. 25, No. 4, pp. 2881–2890 (2010).
31. Laifa, A., and M. Boudour, "Optimal placement and parameter settings of unified power flow controller device using a perturbed particle swarm optimization." *IEEE International Energy Conference and Exhibition*, pp. 205–210 (2010).
32. Fang, W. and H. W. Ngan, "A robust load flow technique for use in power systems with unified power flow controllers," *Electr. Power Syst. Res.*, Vol. 53, No. 3, pp. 181–186 (2000).
33. Bhowmik, A. R., and C. Nandi, "Implementation of unified power flow controller (UPFC) for power quality

improvement in IEEE 14-Bus System," *Int. J. Comp. Tech. Appl*, Vol. 2, No. 6, pp. 1889–1896 (2011).
34. Duman, S., U. Guvenc, Y. Sonmez and N. Yorukeren, "Optimal power flow using gravitational search algorithm," *Energy Conv. Manag.*, Vol. 59, pp. 86–95 (2012).
35. Sakthivel, S. and D. Mary, "Particle swarm optimization algorithm for voltage stability enhancement by optimal reactive power reserve management with multiple TCSCs," *Int. J. Comput. Appl.*, Vol. 11, No. 3 (2010).
36. Yang, X. S., "Bat algorithm for multi-objective optimization." pp. 1–12 (2012).

Bairu Vijay Kumar received a B. Tech degree in Electrical & Electronics Engineering and M. Tech degree in Power Systems Engineering from the National Institute of Technology, Warangal, India, in 2002 and 2008, respectively. He is currently working towards a PhD in Power Systems at the National Institute of Technology, Warangal, India. His current research interest includes enhancement of power system stability using FACTS devices and AI techniques. He is a member of the Institution of Engineers, India.

Nandiraju Venkata Srikanth received a B. Tech degree in Electrical & Electronics Engineering from the College of Engineering, Osmania University, Hyderabad, India, in 1988, and his M. Tech and PhD degrees in Power Systems Engineering from the National Institute of Technology, Warangal, India, in 1999 and 2007, respectively. Currently, he is an Associate Professor in the Department of Electrical Engineering, National Institute of Technology, Warangal, India. He has 25 papers in journals, and international/ national conferences. His areas of research interests include fuzzy logic applications in power systems, power system stabilityand control, HVDC transmission systems, and their impact on power system stability. Dr. Srikanth is an active member in many professional organizations. He is a member of IEEE, a member of the Institution of Engineers, India, and a lifetime member of ISTE.